


 Cite this: *RSC Adv.*, 2025, 15, 26860

Thiazole conjugated amino acid derivatives as potent cytotoxic agents†

 Hieu Trong Le,^a Nguyen Thi Huong Nguyen,^b Quang Vinh Hong,^a Zhuang Qian,^b Thi Minh Bui,^a Linh Nhut Huynh,^a Saw Yu Yu Hnin,^b Zin Paing Htoo,^b An Pham Thuy Le,^b De Quang Tran,^b Hiroyuki Morita^{*b} and Hue Thi Buu Bui^{ID *a}

In the search for anticancer agents, molecular hybridization has gained increasing attention due to its unique advantages like enhanced pharmacological activity, reduced toxicity, and circumvention of drug resistances. In this study, by incorporating amino acids into the thiazole heterocycle scaffold, thirty thiazole–amino acid hybrid derivatives have been successfully synthesized and tested for cytotoxicity against the three human cancer cell lines including lung cancer (A549), cervical cancer (HeLa), and breast cancer (MCF-7) cell lines. The results showed that most of the synthesized hybrid thiazole–amino acids exhibited moderate to good cytotoxicity towards the tested cancer cell lines. Notably, five compounds displayed good cytotoxicity with low IC₅₀ values (2.07–8.51 μM) compared to the positive control 5-fluorouracil (IC₅₀ = 3.49–8.74 μM). These novel thiazole conjugated amino acid derivatives could be considered as lead compounds that merit further optimization and development of anticancer agents.

 Received 21st June 2025
 Accepted 23rd July 2025

DOI: 10.1039/d5ra04425a

rsc.li/rsc-advances

1. Introduction

Molecular hybridization is a strategy in rational drug design, in which novel hybrid molecules are synthesized by combining two or more pharmacophoric units from different potentially bioactive compounds.¹ This technique becomes a powerful tool for developing better treatments for a variety of human diseases, especially cancer.^{2–4} Studies indicated that combination of pharmacological features into a single structure could increase the ability of the resulting molecule to interact with biological targets through dual/multi-target inhibition or new target inhibition, thereby causing synergistic effects to block the multiple oncogenic pathways.^{5–8}

α-Amino acids have been known to play a crucial role in the human body, ranging from building proteins to participating in critical metabolic functions.⁹ These structural features have been commonly employed in drug synthesis and structural modification. Conjugation of pharmacophores and amino acids was reported to produce new hybrid molecules with enhanced pharmacological activity,¹⁰ reduced cytotoxicity,¹¹ and improved water solubility.¹²

Besides, thiazole, a five-membered heterocyclic compound that includes both sulfur and nitrogen, and its derivatives

displayed significant activity against a variety of cancer cell lines.^{13–15} Due to its excellent ability to interact with target proteins,¹⁶ thiazole core is the essential moiety in the structures of many anticancer drugs such as alpelisib, the selective phosphatidylinositol-3 kinase alpha (PI3Kα) inhibitor;¹⁷ dasatinib, the tyrosine kinase inhibitor;¹⁸ dabrafenib, the competitive and selective BRAF inhibitor;¹⁹ epothilone, the microtubule inhibitor;²⁰ and ixabepilone, the microtubule stabilizer.²¹

Thiazole is also known as derivative of cysteine²² or bioisostere of amide.²³ Combination of thiazole moiety and amino acids/peptides was reported to enhance the capability of the resulting hybrid molecules to bind to target proteins and cause strong toxicity against cancer cell lines. For example, thiazole peptidomimetics (thiazole-peptide hybrids) such as largazole²⁴ is a histone deacetylases (HDACs) inhibitor, whereas tubulysin, and pretubulysin,^{25,26} and dolastatin-10,²⁷ have similar mechanism of action, involving the depolymerization of microtubules, arresting cells in the G₂/M phase. However, the structural complexity of thiazole peptidomimetics made them difficult to synthesize including multi-step synthetic procedures and low overall yields.^{26,28–30} In contrast, thiazole–amino acid hybrid with simpler structure such as CKD-516 (prodrug of S516) containing L-valine moiety act as a potent tubulin polymerization inhibitor, and has been progressed to phase 1 clinical trial.³¹

In view of the above findings as well as our continuous research in the field of design and development of small molecules with cytotoxicity potential,^{32–35} we herein report the design and facile synthesis of novel thiazole–amino acid hybrid

^aDepartment of Chemistry, College of Natural Sciences, Can Tho University, Can Tho 900000, Vietnam. E-mail: btbhue@ctu.edu.vn

^bInstitute of Natural Medicine, University of Toyama, 2630-Sugitani, Toyama 930-0194, Japan. E-mail: hmorita@inm.u-toyama.ac.jp

† Electronic supplementary information (ESI) available. See DOI: <https://doi.org/10.1039/d5ra04425a>



derivatives and their *in vitro* cytotoxicities against three human cancer cell lines including lung cancer (A549), cervical cancer (HeLa), and breast cancer (MCF-7) cell lines. The structure–activity relationship (SAR) was analyzed to provide an insight for rational design of more effective thiazole–amino acid hybrids as potent cytotoxic agents.

2. Results and discussion

2.1. Chemical design and synthesis

As shown in Fig. 1, alpelisib (anticancer drug),¹⁷ the CKD-516 (phase 1 clinical trial),³¹ and compound **I**,³⁶ share the common structural features of a thiazole core conjugated with the aromatic ring at the C-4 or C-5 position and the α -amino acid at the C-2 position of the heterocycle ring. Furthermore, the hydrophobic bulky side chains at the *N*-terminal amino acid on

compound **I**,³⁶ and compound **II**,³⁷ could play a critical role in contributing to the observed cytotoxicity by improving the penetration of the molecules through the plasma membrane (Fig. 1). Based on these observations, in this study, the pharmacophore 2-aminothiazole was incorporated with *N*-Boc α -amino acids *via* an amide linkage, in which the Boc (*tert*-butyloxycarbonyl) group was used as the hydrophobic moiety. The phenyl ring with different substituents as well as heterocyclic five/six-membered or the benzimidazolyl moiety was introduced at the C-4 position of the thiazole framework to investigate the structure and activity relationship (SAR) of these novel hybrid structures.

The facile two-step synthetic pathway towards the desired thiazole–amino acid hybrid derivatives is depicted in Scheme 1. We firstly constructed thiazoles **3a–k** with the free amino group at the C-2 position, which served as an anchor to connect to the

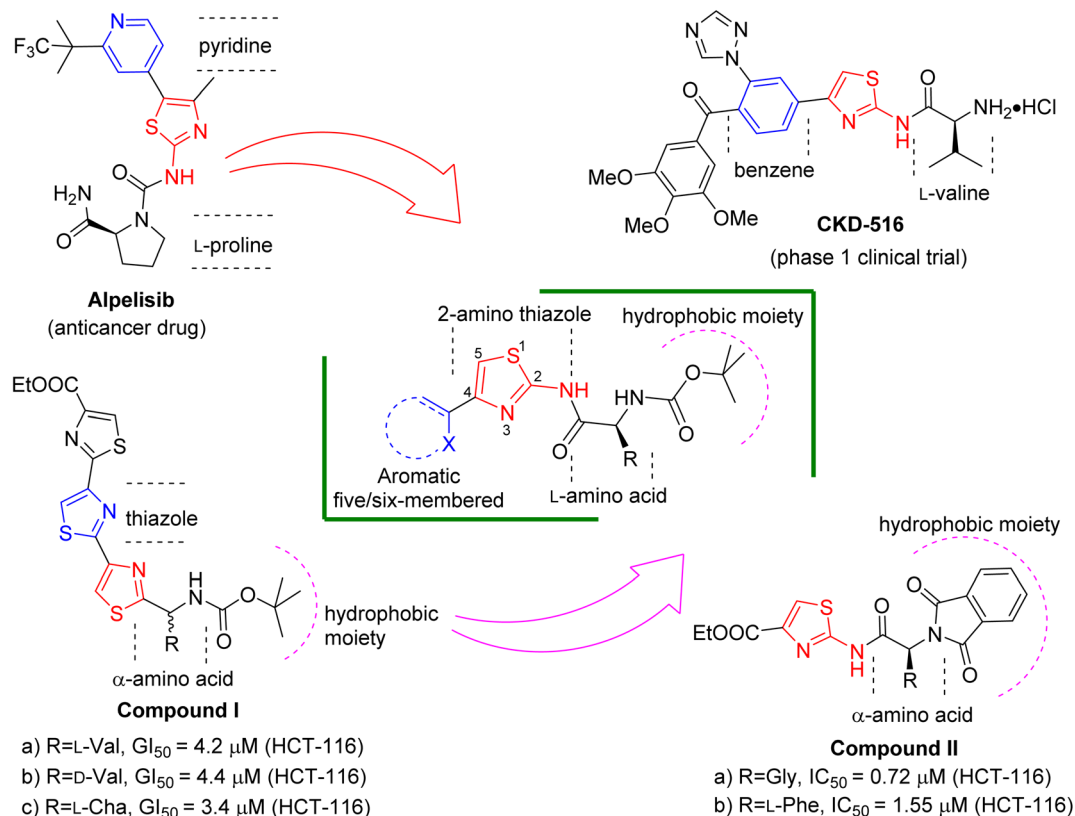
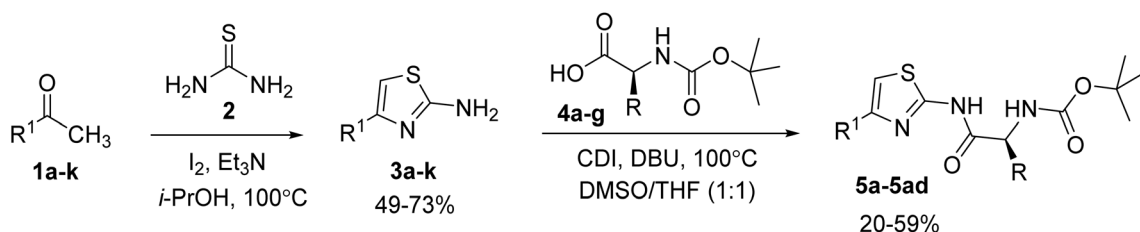


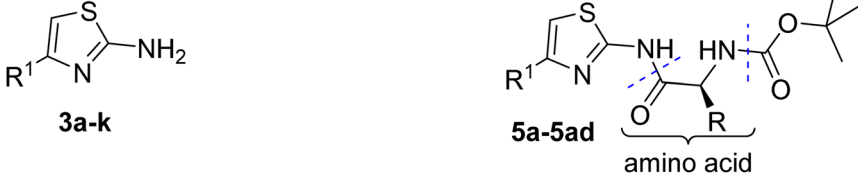
Fig. 1 Rationally designed template for thiazole–amino acid hybrid derivatives.



Scheme 1 Synthesis of thiazole–amino acid hybrid derivatives.



Table 1 Yields and cytotoxicities of the synthesized compounds



| Code | R ¹ | Amino acid | Yield ^a (%) | IC ₅₀ ^b (μM) | | |
|------|------------------------------|------------|------------------------|------------------------------------|--------------------|--------------------|
| | | | | A549 | HeLa | MCF-7 |
| 3a | Ph | — | 73 | >100 | >100 | >100 |
| 3b | 3,4,5-(OMe) ₃ -Ph | — | 60 | >100 | >100 | >100 |
| 3c | 4-Cl-Ph | — | 62 | >100 | 60.35 ± 5.63 | >100 |
| 3d | 4-F-Ph | — | 64 | >100 | >100 | >100 |
| 3e | 4-CF ₃ -Ph | — | 62 | >100 | 38.83 ± 1.65 | >100 |
| 3f | 2,4-(OH) ₂ -Ph | — | 53 | >100 | >100 | >100 |
| 3g | 2-Benzimidazolyl | — | 58 | >100 | >100 | >100 |
| 3h | 2-Furyl | — | 55 | >100 | >100 | >100 |
| 3i | 2-Thiophenyl | — | 57 | >100 | >100 | >100 |
| 3j | 3-Thiophenyl | — | 49 | >100 | >100 | >100 |
| 3k | 2-Pyridyl | — | 52 | >100 | >100 | >100 |
| 5a | Ph | Phe | 49 | 8.02 ± 0.17 | 6.51 ± 0.34 | 6.84 ± 0.11 |
| 5b | Ph | Pro | 43 | >100 | >100 | >100 |
| 5c | Ph | Trp | 41 | 17.61 ± 1.46 | 14.60 ± 0.52 | 16.30 ± 1.31 |
| 5d | Ph | Gly | 42 | 18.43 ± 1.33 | 22.52 ± 2.94 | 37.31 ± 3.68 |
| 5e | Ph | Ala | 59 | 15.07 ± 0.93 | 15.71 ± 0.54 | 51.27 ± 3.01 |
| 5f | Ph | Val | 31 | 2.07 ± 0.10 | 2.16 ± 0.09 | 6.22 ± 0.14 |
| 5g | 3,4,5-(OMe) ₃ -Ph | Phe | 40 | 46.86 ± 0.67 | 45.15 ± 5.36 | 88.11 ± 3.76 |
| 5h | 3,4,5-(OMe) ₃ -Ph | Trp | 27 | 12.57 ± 0.34 | 16.48 ± 0.11 | 16.27 ± 0.56 |
| 5i | 3,4,5-(OMe) ₃ -Ph | Tle | 31 | 24.04 ± 1.99 | >100 | >100 |
| 5j | 4-Cl-Ph | Phe | 52 | >100 | >100 | >100 |
| 5k | 4-Cl-Ph | Trp | 55 | 30.91 ± 0.58 | 24.57 ± 1.04 | 22.01 ± 1.10 |
| 5l | 4-Cl-Ph | Tle | 36 | 14.70 ± 0.69 | 12.23 ± 0.10 | 12.04 ± 0.25 |
| 5m | 4-F-Ph | Phe | 56 | >100 | 61.58 ± 5.86 | >100 |
| 5n | 4-F-Ph | Trp | 43 | 19.28 ± 1.43 | 17.45 ± 0.35 | 24.72 ± 2.02 |
| 5o | 4-F-Ph | Val | 38 | 2.64 ± 0.16 | 3.07 ± 0.07 | 3.92 ± 0.22 |
| 5p | 4-CF ₃ -Ph | Phe | 24 | 82.70 ± 6.48 | 24.14 ± 1.44 | 22.82 ± 1.60 |
| 5q | 4-CF ₃ -Ph | Trp | 20 | 18.73 ± 0.63 | 12.08 ± 0.06 | 13.47 ± 0.29 |
| 5r | 4-CF ₃ -Ph | Tle | 34 | >100 | 17.08 ± 0.88 | 28.17 ± 2.06 |
| 5s | 2,4-(OH) ₂ -Ph | Phe | 29 | 13.35 ± 0.32 | 15.01 ± 0.48 | 16.99 ± 0.53 |
| 5t | 2,4-(OH) ₂ -Ph | Trp | 21 | 12.22 ± 0.39 | 12.59 ± 0.02 | 11.69 ± 0.46 |
| 5u | 2-Benzimidazolyl | Phe | 47 | 11.64 ± 0.06 | 14.92 ± 0.35 | 16.44 ± 0.50 |
| 5v | 2-Benzimidazolyl | Trp | 52 | 22.12 ± 0.92 | 30.75 ± 2.96 | 24.42 ± 0.75 |
| 5w | 2-Furyl | Phe | 24 | 33.37 ± 2.28 | 45.39 ± 4.97 | 34.40 ± 1.88 |
| 5x | 2-Furyl | Trp | 20 | 29.24 ± 0.79 | 29.28 ± 0.60 | 25.63 ± 2.55 |
| 5y | 2-Thiophenyl | Phe | 32 | 31.39 ± 2.67 | 32.45 ± 7.53 | 26.15 ± 1.76 |
| 5z | 2-Thiophenyl | Trp | 47 | 25.23 ± 1.18 | 30.16 ± 1.03 | 22.75 ± 1.24 |
| 5aa | 3-Thiophenyl | Phe | 39 | 14.96 ± 2.31 | 14.55 ± 0.92 | 19.85 ± 2.47 |
| 5ab | 3-Thiophenyl | Trp | 21 | 66.30 ± 2.74 | 57.91 ± 0.80 | 50.31 ± 0.08 |
| 5ac | 2-Pyridyl | Phe | 35 | 4.57 ± 0.39 | 5.41 ± 0.27 | 6.71 ± 0.16 |
| 5ad | 2-Pyridyl | Trp | 30 | 3.68 ± 0.31 | 5.07 ± 0.40 | 8.51 ± 0.74 |
| 5-FU | | | | 3.49 ± 0.25 | 7.59 ± 0.29 | 8.74 ± 0.26 |

^a Isolated yields. ^b IC₅₀: 50% inhibitory concentration. Data are presented as mean ± standard deviation (S.D.) ($n = 3$). Ph: phenyl, Gly: glycine, Ala: alanine, Val: valine, Tle: *tert*-leucine, Pro: proline, Phe: phenylalanine, and Trp: tryptophan.

amino acid moiety, by carrying out the condensation reaction between the commercially available methyl ketones **1a–k** and thiourea **2** using triethylamine as the base and iodine (I₂) as the oxidizing agent.³⁸ Finally, the free amino moiety of **3a–k** were

coupled with the carboxy functionality of the corresponding α -amino acids **4a–g** using 1,1'-carbonyldiimidazole (CDI) as the coupling agent under mild basic conditions,³⁹ to afford the thiazole–amino acid hybrid derivatives **5a–5ad** in moderate



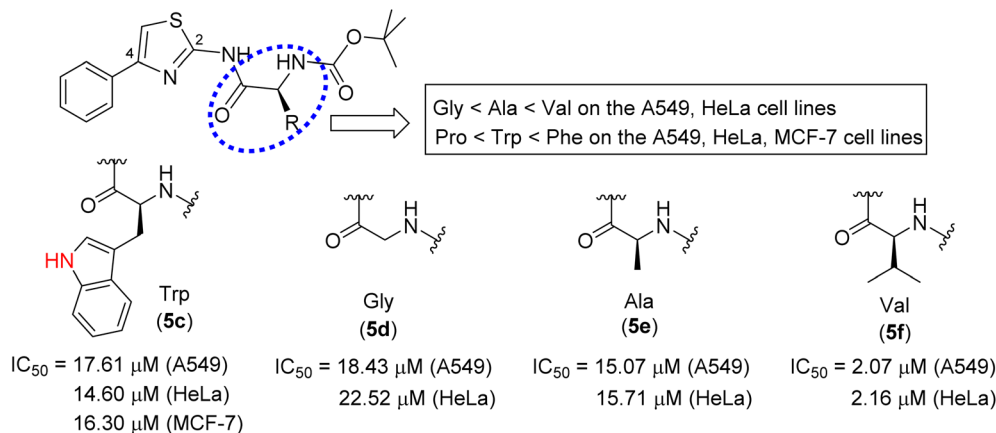


Fig. 2 The SAR of 4-phenylthiazole conjugated amino acid derivatives.

yields (20–59%), in which twenty two derivatives (5g–5i, and 5l–5ad) are novel compounds (Table 1). The structures of the synthesized thiazole–amino acid hybrid derivatives were determined by 1D and 2D NMR, FT-IR, and HR-MS. All compounds were >95% pure according to HPLC spectrometry (see spectra in ESI†).

2.2. Cytotoxicity

All of the synthesized compounds 3a–k and 5a–5ad were tested for their cytotoxicities against the three human cancer cell lines, including lung cancer (A549), cervical cancer (HeLa), and breast cancer (MCF-7) cell lines using MTT assay (Table 1). 5-Fluorouracil (5-FU) was used as the positive control. The results indicated that all 2-aminothiazoles 3a–k showed weak or no cytotoxicity against the tested cancer cell lines at the tested concentration. In contrast, most of the thiazole–amino acid hybrid derivatives exhibited moderate to strong cytotoxicities against the tested three cancer cell lines, except for 5b, 5e, 5g, 5i, 5j, 5m, 5p, and 5ab. Although the cytotoxicity was not observed for the three cancer cell lines, compounds 5e, 5g, and 5p were moderately cytotoxic thiazole–amino acid hybrid derivatives

against two cancer cell lines. Compound 5i also showed moderate cytotoxicity against A549 cell line. These observations clearly demonstrated that the incorporation of amino acids are indeed effective for improving the biological activity of the parent 2-aminothiazoles 3a–k, as indicated by previous reports.^{40,41} Notably, five compounds including 5a (Ph, Phe), 5f (Ph, Val), 5o (4-F-Ph, Val), 5ac (2-pyridyl, Phe), and 5ad (2-pyridyl, Trp) exhibited equal or stronger activities, compared to the positive control 5-FU (IC₅₀ values of 3.49, 7.59, and 8.74 μM against A549, HeLa, and MCF-7, respectively). In detailed, hybrid compound 5a showed strong activity against A549, HeLa, and MCF-7 cell lines with IC₅₀ values of 8.02, 6.51, and 6.84 μM, respectively, in which later two were stronger than those of 5-FU; two thiazole–valine hybrids 5f and 5o exhibited better cytotoxicities than 5-FU towards the A549, HeLa, and MCF-7; two compounds 5ac (IC₅₀ = 4.57–6.71 μM) and 5ad (IC₅₀ = 3.68–8.51 μM) with the 2-pyridyl substituent at the C-4 position of the thiazole core displayed equal cytotoxicity to those of 5-FU (IC₅₀ = 3.49–8.74 μM). Generally, the thiazole–tryptophan hybrids exhibited more potent cytotoxicity than the corresponding thiazole–phenylalanine hybrids, except for 5c, 5v, and

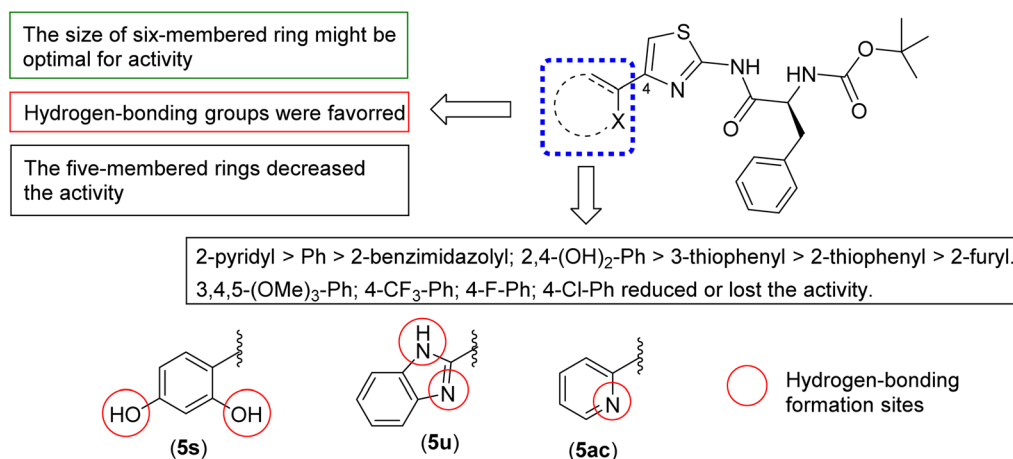


Fig. 3 The SAR of the thiazole–phenylalanine hybrid series.



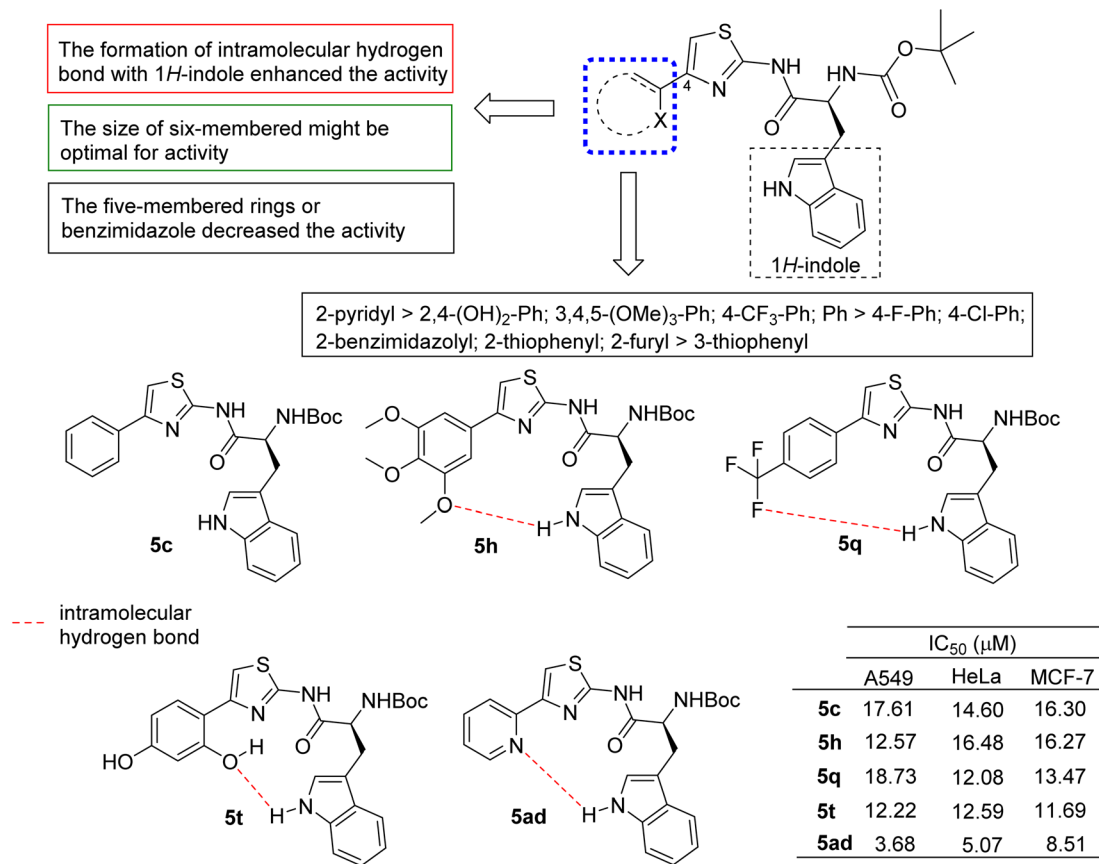


Fig. 4 The SAR of the thiazole–tryptophan hybrid series.

5ab. The higher activity is probably due to the good interaction of the 1*H*-indole moiety with the target protein.⁴²

To further clarify the SAR of the synthesized compounds, we carried out the SAR analysis. To this end, we firstly analyzed the SAR of **5a**–**5f**, all of which have the phenyl ring at the C-4 position with several amino acids including glycine (Gly), alanine (Ala), valine (Val), proline (Pro), phenylalanine (Phe), and tryptophan (Trp) at the C-2 position of the thiazole framework, respectively (Fig. 2). The SAR analysis should clearly summarize that the activities of **5d**, **5e**, **5f** against A549 and HeLa cell lines increased with the side chain size of Gly, Ala, and Val. However, the introduction of the further bulkier benzene ring (**5a**) or the 1*H*-indole moiety (**5c**) than Gly, Ala, and Val led to decrease the activity, compared to **5f**, suggesting that the appropriate size of the side chain would be required to significantly enhance the activity. However, the SAR analysis simultaneously suggested that this may be ruled out when hydrogen bond interaction of the side chain of the compound was formed with the target proteins, since **5c** with an N atom on the side chain^{43,44} showed the comparable activity to those of **5d** and **5e**, whereas **5b** completely lost the activity. Thus, both the size and flexibility of the side chain of the amino acids at the C-2 position were closely correlated to the activity.

Next, we analyzed the effect of the nature of the substituents at the C-4 position of the thiazole framework on the cytotoxic activity. For the thiazole–phenylalanine hybrid series (Fig. 3),

the presence of the aromatic six-membered ring with no substituent (**5a**) displayed good activity. Further introduction of large groups such as 3,4,5-(OMe)₃ (**5g**) or 4-CF₃ (**5p**) on the benzene ring led to decreased activity. In addition, substitution of the phenyl group of **5a** with aromatic five-membered rings such as furyl (**5w**) and thiophenyl (**5y** and **5aa**) also decreased the activity. Notably, **5ac** with the six-membered pyridine ring containing the nitrogen atom capable of forming a hydrogen bond exhibited almost 2-fold stronger activity against the A549 cell line, as compared to that of **5a**, while it still remained the same activity with those of **5a** towards the HeLa and MCF-7. Both the size and the ability of forming hydrogen bonding of the substituent seemed to play a significant role in determining the activity, as clearly observed in the cases of **5s** and **5u**, compared to **5g** and **5p**. The presence of the weak hydrogen bonding group such as 4-Cl (**5j**) or the strong electron withdrawing group such as 4-F (**5m**) likely contributed to the observed decreased activity.

In contrast, the presence of the 4-F group on the benzene ring at the C-4 position of the thiazole heterocycle in conjunction with the valine moiety at the C-2 (**5o**) resulted in 1.6-fold increase in the activity against the MCF-7, compared to that of the unsubstituted analog **5f**, while it maintained almost the same activity against the A549 and HeLa cell lines as those of **5f**. Meanwhile, within the three compounds of the thiazole-Trp series, the presence of the 4-Cl group on the benzene ring at



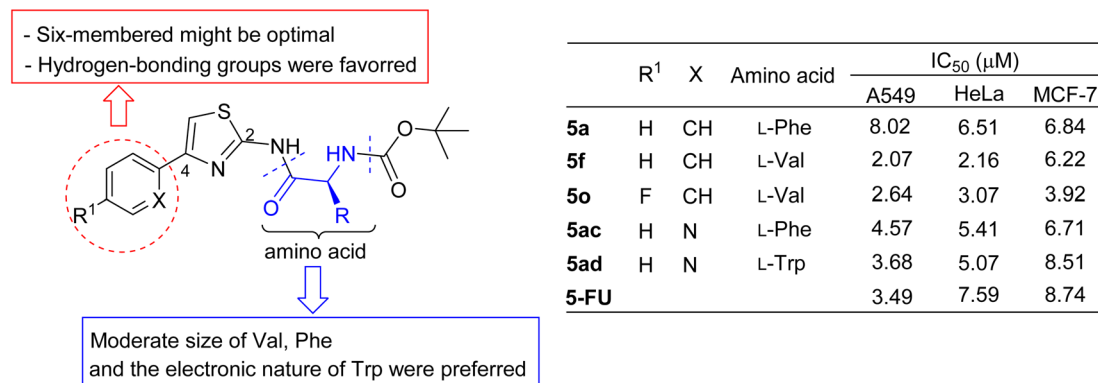


Fig. 5 Structure–potent cytotoxic relationship of the thiazole–amino acid hybrids.

the C-4 position (**5l**) gave rise to better activity, compared to the large 3,4,5-(OMe)₃ (**5i**) and 4-CF₃ groups (**5r**).

Finally, SAR analysis of the thiazole-tryptophan hybrid series (Fig. 4) revealed that the six-membered rings at the C-4 position were more preferred than the five-membered rings or the benzimidazole ring. Notedly, the presence of the NH group on the Trp moiety likely reduce the size limitation of the 3,4,5-(OMe)₃ group (the activity of **5h** against **5g** and **5i**), the 4-CF₃ group (the activity of **5q** against **5p** and **5r**), or the 2,4-(OH)₂ group (the activity of **5t** against **5s**). The reason could be due to the formation of an intramolecular hydrogen-bonding between the NH group on the Trp and the hydrogen acceptors such as OMe, CF₃, and OH groups. Similarly, **5ad** with the N atom on the pyridine ring could form the hydrogen bond with NH group on the Trp, which resulted in bearing its 1.9- to 4.8-fold stronger activity than **5c**. In fact, the intramolecular hydrogen-bonding reportedly improved not only the lipophilicity (closed form), but also the hydrophilicity (open form), thereby increasing accessibility to target proteins.^{45,46} Moreover, the intramolecular hydrogen-bonding could result in forming rigid conformation of the molecules, thereby favoring their arrangement in protein pockets.^{47,48}

In summary, the observed strong cytotoxicities of the thiazole–amino acid hybrid derivatives **5a**, **5f**, **5o**, **5ac**, and **5ad** towards the A549, HeLa, and MCF-7 cell lines were crucially attributed to the size and the electron donating/accepting nature of the substituents on the six-membered rings at the C-4 position as well as the side chain of the amino acid moieties at the C-2 position of the thiazole core (Fig. 5). Notedly, the presence of the N atom (hydrogen-bonding formation site) on the pyridine⁴⁹ moiety at the C-4 position or on the tryptophan^{50,51} moiety at the C-2 position significantly enhanced the activity. These structures provide new thiazole–amino acid hybrid derivatives as potential leads for further optimization and development of novel anticancer compounds. Further studies on the synthesis and cytotoxicities of other hydrophobic, unnatural amino acid side chains and different *N*-protected amino acids as well as the mechanism of the activities have been continuing in our lab and the results will be reported in the near future.

3. Conclusions

Thirty thiazole conjugated amino acid derivatives have been designed and successfully synthesized. Most of the compounds displayed moderate to strong cytotoxicity against the three tested human cancer cell lines A549, HeLa, and MCF-7. Remarkably, five compounds **5a**, **5f**, **5o**, **5ac**, and **5ad** exhibited comparable to stronger cytotoxic activities, compared to the positive control 5-FU. These novel structures could be considered as promising leads for further studies for the development of novel anticancer drugs.

4. Experimental section

4.1 Chemistry

Reactions were monitored by thin layer chromatography (TLC) on 0.2 mm pre-coated silica gel 60 F254 plates (Merck). Melting points (Mp, °C) were recorded on an INE-X-4 melting point apparatus with microscope and were uncorrected. NMR spectra were measured with Bruker Avance 600 (¹H, 600 MHz; ¹³C, 150 MHz) and JEOL 400 (¹H, 400 MHz; ¹³C, 100 MHz) spectrometers using DMSO-*d*₆ as solvent. HSQC, HMBC, and COSY spectra were recorded by a JEOL 400 MHz spectrometer. High resolution electrospray ionization (HRESI)-MS data were performed on Agilent 6530 qTOF, X500R QTOF, and Thermo Scientific LTQ Orbitrap XL ETD spectrometers. Fourier transform (FT)-IR was conducted using the KBr pellet method on a JASCO FT/IR 4600 spectrometer. Chemical shifts are given in parts per million (ppm) relative to tetramethylsilane (Me₄Si, δ = 0); *J* values are given in Hertz. Silica gel 60 (0.063–0.200 mm, Merck) was used for column chromatography. All chemicals and solvents used in this study were of analytical grade. Purity of the compounds that were synthesized and used for the cytotoxic assay were estimated, based on the peak area of the compounds on the HPLC chromatograms, using an Agilent Infinity II 1260 HPLC system coupled with a SUPELCO Discovery C18 (4.6 × 250 mm) column (Flow rate; 0.5 mL min⁻¹, mobile phase; water and MeOH, both containing 0.1% formic acid; 0–40 min: 50 to 100% MeOH, UV; 190 to 400 nm).

4.2. General procedure for preparation of compounds 3a–k

A mixture of methyl ketones **1a–k** (5 mmol), thiourea (**2**) (761 mg, 10 mmol), and iodine (1904 mg, 7.5 mmol) was



dissolved in 10 mL of isopropanol and 0.5 mL of triethylamine was then added. The resulting mixture was stirred at 100 °C for 6–10 hours. The reaction progress was monitored by TLC. At the end of the reaction, the mixture was cooled to room temperature, and the excess iodine was removed by using the saturated aqueous solution of Na₂S₂O₃. The pH of the mixture was adjusted to 7–8 by using an aqueous NH₃ solution. The mixture was extracted with ethyl acetate (3 × 50 mL). The combined organic layers were washed with 50 mL of a saturated aqueous NaCl solution, dried over anhydrous Na₂SO₄, and the solvent was then evaporated under reduced pressure to produce the crude product. Column chromatography of the crude product provided the desired compounds **3a–k**.

4.3. 4-Phenylthiazol-2-amine (3a)

White solid. Yield: 642 mg (73%). Mp 146–148 °C. ¹H-NMR (400 MHz, DMSO-*d*₆, δ ppm): 7.80–7.78 (m, 2H), 7.38–7.33 (m, 2H), 7.27–7.23 (m, 1H), 7.06 (s, 2H), 7.00 (s, 1H). ¹³C-NMR (100 MHz, DMSO-*d*₆, δ ppm): 168.1, 149.7, 134.8, 128.4, 127.1, 125.4, 101.4.

4.4. 4-(3,4,5-Trimethoxyphenyl)thiazol-2-amine (3b)

White solid. Yield: 799 mg (60%). Mp 168–170 °C. ¹H-NMR (400 MHz, DMSO-*d*₆, δ ppm): 7.09 (s, 2H), 7.08 (s, 2H), 7.01 (s, 1H), 3.81 (s, 6H), 3.66 (s, 3H). ¹³C-NMR (100 MHz, DMSO-*d*₆, δ ppm): 168.5, 153.4, 150.3, 137.4, 131.2, 103.4, 101.6, 60.6, 56.3.

4.5. 4-(4-Chlorophenyl)thiazol-2-amine (3c)

White solid. Yield: 652 mg (62%). Mp 162–164 °C. ¹H-NMR (400 MHz, DMSO-*d*₆, δ ppm): 7.82–7.79 (m, 2H), 7.43–7.40 (m, 2H), 7.10 (s, 2H), 7.08 (s, 1H). ¹³C-NMR (100 MHz, DMSO-*d*₆, δ ppm): 168.2, 148.4, 133.6, 131.4, 128.4, 127.1, 102.2.

4.6. 4-(4-Fluorophenyl)thiazol-2-amine (3d)

White solid. Yield: 620 mg (64%). Mp 122–124 °C. ¹H-NMR (400 MHz, DMSO-*d*₆, δ ppm): 7.85–7.80 (m, 2H), 7.22–7.16 (m, 2H), 7.08 (s, 2H), 6.98 (s, 1H). ¹³C-NMR (100 MHz, DMSO-*d*₆, δ ppm): 168.2, 162.5, 160.1, 148.7, 131.5, 131.4, 127.4, 127.3, 115.3, 115.1, 101.1. HR-ESI-MS (*m/z*): [M + H]⁺ calcd for C₉H₈FN₂S, 195.0387; found, 195.0383.

4.7. 4-(4-(Trifluoromethyl)phenyl)thiazol-2-amine (3e)

White solid. Yield: 755 mg (62%). Mp 184–186 °C. ¹H-NMR (400 MHz, DMSO-*d*₆, δ ppm): 8.01 (d, *J* = 8.1 Hz, 2H), 7.72 (d, *J* = 8.3 Hz, 2H), 7.26 (s, 1H), 7.18 (s, 2H). ¹³C-NMR (100 MHz, DMSO-*d*₆, δ ppm): 168.4, 148.2, 138.5, 127.3, 125.9, 125.4, 125.4, 123.0, 104.3.

4.8. 4-(2-Aminothiazol-4-yl)benzene-1,3-diol (3f)

White solid. Yield: 547 mg (53%). Mp 180–182 °C. ¹H-NMR (400 MHz, DMSO-*d*₆, δ ppm): 11.95 (s, 1H), 9.44 (s, 1H), 7.47 (d, *J* = 8.5 Hz, 1H), 7.40 (s, 2H), 6.77 (s, 1H), 6.25 (dd, *J* = 2.4, 8.5 Hz, 1H), 6.20 (d, *J* = 2.4 Hz, 1H). ¹³C-NMR (100 MHz, DMSO-*d*₆, δ ppm): 168.2, 158.3, 156.8, 147.5, 127.1, 110.2, 107.0, 102.8, 97.0.

4.9. 4-(1*H*-Benzo[*d*]imidazole-2-yl)thiazol-2-amine (3g)

Yellow solid. Yield: 627 mg (58%). Mp 208–210 °C. ¹H-NMR (400 MHz, DMSO-*d*₆, δ ppm): 12.48 (s, 1H), 7.52 (s, 2H), 7.33 (s, 1H), 7.17–7.13 (m, 4H). ¹³C-NMR (100 MHz, DMSO-*d*₆, δ ppm): 168.8, 147.7, 141.9, 121.6, 106.9. HR-ESI-MS (*m/z*): [M + H]⁺ calcd for C₁₀H₉N₄S, 217.0542; found, 217.0538.

4.10. 4-(Furan-2-yl)thiazol-2-amine (3h)

Light brown solid. Yield: 453 mg (55%). Mp 104–106 °C. ¹H-NMR (400 MHz, DMSO-*d*₆, δ ppm): 7.64 (t, *J* = 1.3 Hz, 1H), 7.13 (s, 2H), 6.71 (s, 1H), 6.52–6.51 (m, 2H). ¹³C-NMR (100 MHz, DMSO-*d*₆, δ ppm): 168.5, 150.4, 142.1, 141.6, 111.4, 105.8, 100.4.

4.11. 4-(Thiophen-2-yl)thiazol-2-amine (3i)

Yellow solid. Yield: 520 mg (57%). Mp 117–119 °C. ¹H-NMR (400 MHz, DMSO-*d*₆, δ ppm): 7.40 (dd, *J* = 1.1, 5.0 Hz, 1H), 7.37 (dd, *J* = 1.1, 3.7 Hz, 1H), 7.15 (s, 2H), 7.04 (dd, *J* = 3.7, 5.0 Hz, 1H), 6.85 (s, 1H). ¹³C-NMR (100 MHz, DMSO-*d*₆, δ ppm): 168.2, 144.4, 139.1, 127.7, 124.6, 122.6, 99.6.

4.12. 4-(Thiophen-3-yl)thiazol-2-amine (3j)

Yellow solid. Yield: 446 mg (49%). Mp 127–129 °C. ¹H-NMR (400 MHz, DMSO-*d*₆, δ ppm): 7.61 (dd, *J* = 1.2, 3.1 Hz, 1H), 7.52 (dd, *J* = 3.1, 5.0 Hz, 1H), 7.45 (dd, *J* = 1.2, 5.0 Hz, 1H), 7.05 (s, 2H), 6.84 (s, 1H). ¹³C-NMR (100 MHz, DMSO-*d*₆, δ ppm): 168.1, 146.3, 137.2, 126.4, 125.8, 120.7, 101.0. HR-ESI-MS (*m/z*): [M + H]⁺ calcd for C₇H₇N₂S₂, 183.0045; found, 183.0043.

4.13. 4-(Pyridin-2-yl)thiazol-2-amine (3k)

Purple solid. Yield: 463 mg (52%). Mp 153–155 °C. ¹H-NMR (400 MHz, DMSO-*d*₆, δ ppm): 8.53 (dt, *J* = 1.5, 4.8 Hz, 1H), 7.84–7.79 (m, 2H), 7.29–7.23 (m, 2H), 7.13 (s, 2H). ¹³C-NMR (100 MHz, DMSO-*d*₆, δ ppm): 168.4, 152.3, 150.0, 149.2, 137.0, 122.2, 120.0, 105.3.

4.14. General procedure for preparation of compounds **5a–5ad**

A mixture of 4-substituted thiazol-2-amine (**3a–k**) (1 mmol), *N*-Boc amino acids (**4a–g**) (1.2 mmol), CDI (194.58 mg, 1.2 mmol), and 1,8-diazabicyclo[5.4.0]undec-7-ene (DBU, 76.12 mg, 0.5 mmol) was dissolved in 1 mL of solvent system (THF : DMSO = 1 : 1). The mixture was stirred at room temperature for 10 minutes and then at 100 °C for 8–12 hours. The reaction progress was monitored by TLC. At the end of the reaction, the mixture was extracted with ethyl acetate (3 × 20 mL). The combined organic layers were sequentially washed with 20 mL of saturated aqueous solution of NH₄Cl; 20 mL of saturated aqueous solution of NaHCO₃; and 20 mL of saturated aqueous solution of NaCl. The organic layer was dried over anhydrous Na₂SO₄ and evaporated under reduced pressure to obtain the crude product. Column chromatography of the crude product provided the corresponding thiazole-amino acid hybrids (**5a–5ad**).



4.15. *tert*-Butyl (S)-(1-oxo-3-phenyl-1-((4-phenylthiazol-2-yl)amino)propan-2-yl)carbamate (5a)

White solid. Yield: 207 mg (49%). Mp 129–131 °C. FT-IR (KBr) ν_{\max} (cm⁻¹): 3258, 3067, 2979, 1705, 1662, 1551, 1297, 1169, 743, 708. ¹H-NMR (400 MHz, DMSO-*d*₆, δ ppm): 12.52 (s, 1H), 7.91 (d, *J* = 7.2 Hz, 2H), 7.65 (s, 1H), 7.44 (t, *J* = 7.6 Hz, 2H), 7.38–7.27 (m, 6H), 7.21 (t, *J* = 7.2 Hz, 1H), 4.50–4.44 (m, 1H), 3.04 (dd, *J* = 4.1, 13.6 Hz, 1H), 2.83 (dd, *J* = 10.8, 13.4 Hz, 1H), 1.32 (s, 9H). ¹³C-NMR (100 MHz, DMSO-*d*₆, δ ppm): 171.3, 157.7, 155.4, 148.8, 137.6, 134.2, 129.3, 128.7, 128.0, 127.8, 126.3, 125.6, 108.1, 78.2, 55.9, 36.9, 28.1. HR-ESI-MS (*m/z*): [M + H]⁺ calcd for C₂₃H₂₆N₃O₃S, 424.1689; found, 424.1659.

4.16. *tert*-Butyl (S)-2-((4-phenylthiazol-2-yl)carbamoyl)pyrrolidine-1-carboxylate (5b)

White solid. Yield: 160 mg (43%). Mp 208–210 °C. FT-IR (KBr) ν_{\max} (cm⁻¹): 3171, 3064, 2981, 1703, 1659, 1558, 1425, 1279, 1170, 852, 774, 722. ¹H-NMR (600 MHz, DMSO-*d*₆, δ ppm): 12.40 (s, 1H), 7.90 (dd, *J* = 1.2, 8.4 Hz, 2H), 7.62 (d, *J* = 1.8 Hz, 1H), 7.43 (t, *J* = 7.8 Hz, 2H), 7.37–7.31 (m, 1H), 4.44–4.37 (m, 1H), 3.46–3.44 (m, 1H), 3.37–3.34 (m, 1H), 2.25–2.20 (m, 1H), 1.93–1.86 (m, 2H), 1.84–1.80 (m, 1H), 1.40 (s, 3H), 1.25 (s, 6H). ¹³C-NMR (150 MHz, DMSO-*d*₆, δ ppm): 171.9, 171.4, 157.8, 153.5, 152.8, 148.9, 134.2, 128.7, 128.4, 127.7, 125.6, 125.5, 108.2, 108.0, 101.4, 78.8, 78.7, 59.3, 59.1, 46.7, 46.5, 30.8, 30.0, 28.1, 27.8, 24.0, 23.4. HR-ESI-MS (*m/z*): [M + H]⁺ calcd for C₁₉H₂₄N₃O₃S, 374.1538; found, 374.1594.

4.17. *tert*-Butyl (S)-(3-(1*H*-indol-3-yl)-1-oxo-1-((4-phenylthiazol-2-yl)amino)propan-2-yl)carbamate (5c)

White solid. Yield: 190 mg (41%). Mp 193–195 °C. FT-IR (KBr) ν_{\max} (cm⁻¹): 3412, 3339, 3276, 2976, 2924, 1700, 1664, 1549, 1511, 1368, 1251, 1162, 848, 735. ¹H-NMR (400 MHz, DMSO-*d*₆, δ ppm): 10.85 (s, 1H), 7.91 (d, *J* = 7.2 Hz, 2H), 7.75 (d, *J* = 7.8 Hz, 1H), 7.64 (s, 1H), 7.44 (t, *J* = 7.7 Hz, 2H), 7.35–7.31 (m, 2H), 7.21 (d, *J* = 1.8 Hz, 1H), 7.15 (d, *J* = 7.7 Hz, 1H), 7.06 (t, *J* = 7.3 Hz, 1H), 6.98 (t, *J* = 7.3 Hz, 1H), 4.52 (q, *J* = 8.5 Hz, 1H), 3.16 (dd, *J* = 5.2, 14.4 Hz, 1H), 3.00 (dd, *J* = 9.5, 14.4 Hz, 1H), 1.32 (s, 9H). ¹³C-NMR (100 MHz, DMSO-*d*₆, δ ppm): 171.7, 157.8, 155.2, 148.8, 135.9, 134.2, 128.7, 127.7, 127.1, 125.6, 124.1, 120.8, 118.7, 118.1, 111.2, 109.4, 108.1, 78.2, 55.0, 28.1, 27.6, 27.4. HR-ESI-MS (*m/z*): [M + H]⁺ calcd for C₂₅H₂₇N₄O₃S, 463.1798; found, 463.1778.

4.18. *tert*-Butyl (2-oxo-2-((4-phenylthiazol-2-yl)amino)ethyl)carbamate (5d)

White solid. Yield: 139 mg (42%). Mp 159–161 °C. FT-IR (KBr) ν_{\max} (cm⁻¹): 3408, 3238, 3102, 2979, 2931, 1674, 1554, 1508, 1268, 1167, 859, 729. ¹H-NMR (400 MHz, DMSO-*d*₆, δ ppm): 12.31 (s, 1H), 7.90 (dd, *J* = 1.2, 8.4 Hz, 2H), 7.63 (s, 1H), 7.43 (t, *J* = 7.6 Hz, 2H), 7.35–7.31 (m, 1H), 7.19 (t, *J* = 6.1 Hz, 1H), 3.87 (d, *J* = 6.2 Hz, 2H), 1.40 (s, 9H). ¹³C-NMR (100 MHz, DMSO-*d*₆, δ ppm): 168.8, 157.8, 155.9, 148.8, 134.3, 128.8, 127.8, 125.7, 108.1, 78.3, 43.0, 28.2. HR-ESI-MS (*m/z*): [M + H]⁺ calcd for C₁₆H₂₀N₃O₃S, 334.1220; found, 334.1210.

4.19. *tert*-Butyl (S)-(1-oxo-1-((4-phenylthiazol-2-yl)amino)propan-2-yl)carbamate (5e)

White solid. Yield: 204 mg (59%). Mp 143–145 °C. FT-IR (KBr) ν_{\max} (cm⁻¹): 3337, 3252, 3217, 3091, 2981, 1710, 1673, 1554, 1496, 1269, 1163, 1022, 852, 745. ¹H-NMR (400 MHz, DMSO-*d*₆, δ ppm): 12.32 (s, 1H), 7.91 (dd, *J* = 1.1, 8.3 Hz, 2H), 7.64 (s, 1H), 7.46–7.42 (m, 2H), 7.35–7.31 (m, 1H), 7.28 (d, *J* = 7.1 Hz, 1H), 4.27 (q, *J* = 7.1 Hz, 1H), 1.39 (s, 9H), 1.28 (s, 3H). ¹³C-NMR (100 MHz, DMSO-*d*₆, δ ppm): 172.4, 157.9, 155.2, 148.9, 134.3, 128.8, 127.8, 125.7, 108.2, 78.2, 49.7, 28.2, 17.6. HR-ESI-MS (*m/z*): [M + H]⁺ calcd for C₁₇H₂₂N₃O₃S, 348.1376; found, 348.1378.

4.20. *tert*-Butyl (S)-(3-methyl-1-oxo-1-((4-phenylthiazol-2-yl)amino)butan-2-yl)carbamate (5f)

White solid. Yield: 116 mg (31%). Mp 101–103 °C. FT-IR (KBr) ν_{\max} (cm⁻¹): 3293, 3191, 3075, 2969, 1667, 1556, 1376, 1274, 1166, 1023, 846, 773, 716. ¹H-NMR (400 MHz, DMSO-*d*₆, δ ppm): 12.31 (s, 1H), 7.91–7.89 (m, 2H), 7.63 (s, 1H), 7.44 (t, *J* = 7.6 Hz, 2H), 7.33 (t, *J* = 7.3 Hz, 1H), 7.11 (d, *J* = 8.2 Hz, 1H), 4.08 (t, *J* = 7.8 Hz, 1H), 2.05–2.00 (m, 1H), 1.39 (s, 9H), 0.89 (t, *J* = 5.9 Hz, 6H). ¹³C-NMR (100 MHz, DMSO-*d*₆, δ ppm): 171.2, 157.5, 155.5, 148.8, 134.2, 128.6, 127.7, 125.6, 108.1, 78.2, 59.7, 29.9, 28.1, 18.9, 18.4. HR-ESI-MS (*m/z*): [M + H]⁺ calcd for C₁₉H₂₆N₃O₃S, 376.1689; found, 376.1696.

4.21. *tert*-Butyl (S)-(1-oxo-3-phenyl-1-((4-(3,4,5-trimethoxyphenyl)thiazol-2-yl)amino)propan-2-yl)carbamate (5g)

White solid. Yield: 206 mg (40%). Mp 216–218 °C. FT-IR (KBr) ν_{\max} (cm⁻¹): 3305, 3251, 3216, 2968, 2931, 1666, 1547, 1255, 1166, 1123, 1018, 849, 737. ¹H-NMR (400 MHz, DMSO-*d*₆, δ ppm): 12.54 (s, 1H), 7.67 (s, 1H), 7.38 (d, *J* = 7.2 Hz, 2H), 7.29 (t, *J* = 7.4 Hz, 3H), 7.22 (d, *J* = 4.3 Hz, 3H), 4.50–4.44 (m, 1H), 3.85 (s, 6H), 3.69 (s, 3H), 3.04 (dd, *J* = 4.0, 13.5 Hz, 1H), 2.82 (dd, *J* = 10.9, 13.4 Hz, 1H), 1.31 (s, 9H). ¹³C-NMR (100 MHz, DMSO-*d*₆, δ ppm): 171.5, 157.6, 155.5, 153.1, 148.9, 137.8, 137.3, 130.0, 129.4, 128.1, 126.4, 107.9, 103.0, 78.3, 60.1, 56.1, 55.9, 37.0, 28.2. HR-ESI-MS (*m/z*): [M + H]⁺ calcd for C₂₆H₃₂N₃O₆S, 514.2006; found, 514.1993.

4.22. *tert*-Butyl (S)-(3-(1*H*-indol-3-yl)-1-oxo-1-((4-(3,4,5-trimethoxyphenyl)thiazol-2-yl)amino)propan-2-yl)carbamate (5h)

White solid. Yield: 148 mg (27%). Mp 132–134 °C. FT-IR (KBr) ν_{\max} (cm⁻¹): 3342, 3206, 3096, 2968, 2936, 2839, 1685, 1555, 1496, 1420, 1338, 1240, 1164, 1124, 847, 740. ¹H-NMR (400 MHz, DMSO-*d*₆, δ ppm): 12.55 (s, 1H), 10.85 (s, 1H), 7.76 (d, *J* = 7.8 Hz, 1H), 7.66 (s, 1H), 7.33 (d, *J* = 8.0 Hz, 1H), 7.21 (s, 3H), 7.14 (d, *J* = 7.7 Hz, 1H), 7.06 (t, *J* = 7.4 Hz, 1H), 6.98 (t, *J* = 7.4 Hz, 1H), 4.54–4.48 (m, 1H), 3.84 (s, 6H), 3.69 (s, 3H), 3.15 (dd, *J* = 5.2, 14.0 Hz, 1H), 3.00 (dd, *J* = 9.5, 14.4 Hz, 1H), 1.32 (s, 9H). ¹³C-NMR (100 MHz, DMSO-*d*₆, δ ppm): 171.9, 157.7, 155.3, 153.1, 148.8, 137.3, 136.1, 130.0, 127.2, 124.3, 120.9, 118.9, 118.2, 111.3, 109.5, 107.9, 103.0, 78.3, 60.1, 55.9, 55.2, 28.2, 27.5. HR-ESI-MS (*m/z*): [M + H]⁺ calcd for C₂₈H₃₃N₄O₆S, 553.2115; found, 553.2110.



4.23. *tert*-Butyl (S)-(3,3-dimethyl-1-oxo-1-((4-(3,4,5-trimethoxyphenyl)thiazol-2-yl)amino)butan-2-yl)carbamate (5i)

White solid. Yield: 149 mg (31%). Mp 181–183 °C. FT-IR (KBr) ν_{\max} (cm⁻¹): 3337, 3196, 3083, 2966, 2834, 1675, 1552, 1500, 1408, 1333, 1240, 1165, 1124, 1003, 852, 730. ¹H-NMR (600 MHz, DMSO-*d*₆, δ ppm): 12.29 (s, 1H), 7.64 (s, 1H), 7.20 (s, 2H), 6.92 (d, *J* = 7.8 Hz, 1H), 4.20 (d, *J* = 7.8 Hz, 1H), 3.84 (s, 6H), 3.69 (s, 3H), 1.39 (s, 9H), 0.97 (s, 9H). ¹³C-NMR (150 MHz, DMSO-*d*₆, δ ppm): 157.2, 155.5, 153.1, 148.9, 137.4, 130.0, 107.8, 103.2, 78.4, 62.1, 60.1, 55.9, 33.9, 28.1, 26.5. HR-ESI-MS (*m/z*): [M + H]⁺ calcd for C₂₃H₃₄N₃O₆S, 480.2163; found, 480.2177.

4.24. *tert*-Butyl (S)-(1-((4-(4-chlorophenyl)thiazol-2-yl)amino)-1-oxo-3-phenylpropan-2-yl)carbamate (5j)

White solid. Yield: 236 mg (52%). Mp 160–162 °C. FT-IR (KBr) ν_{\max} (cm⁻¹): 3342, 3205, 3089, 2977, 2928, 1680, 1544, 1276, 1163, 1085, 1020, 838, 741, 696. ¹H-NMR (400 MHz, DMSO-*d*₆, δ ppm): 12.54 (s, 1H), 7.93 (d, *J* = 8.6 Hz, 2H), 7.71 (d, *J* = 0.6 Hz, 1H), 7.51 (d, *J* = 8.7 Hz, 2H), 7.37 (d, *J* = 7.0 Hz, 2H), 7.30 (q, *J* = 7.2 Hz, 3H), 7.23–7.19 (m, 1H), 4.50–4.44 (m, 1H), 3.04 (dd, *J* = 4.4, 13.5 Hz, 1H), 2.83 (dd, *J* = 10.6, 13.7 Hz, 1H), 1.32 (s, 9H). ¹³C-NMR (100 MHz, DMSO-*d*₆, δ ppm): 171.4, 157.9, 155.4, 147.6, 137.6, 133.0, 132.2, 129.2, 128.7, 128.0, 127.3, 126.3, 108.9, 78.2, 55.9, 36.8, 28.0. HR-ESI-MS (*m/z*): [M + H]⁺ calcd for C₂₃H₂₅ClN₃O₃S, 458.1300; found, 458.1319.

4.25. *tert*-Butyl (S)-(1-((4-(4-chlorophenyl)thiazol-2-yl)amino)-3-(1*H*-indol-3-yl)-1-oxopropan-2-yl)carbamate (5k)

White solid. Yield: 273 mg (55%). Mp 189–191 °C. FT-IR (KBr) ν_{\max} (cm⁻¹): 3424, 3362, 3057, 2978, 2927, 1688, 1541, 1274, 1164, 1087, 1019, 838, 740, 606. ¹H-NMR (400 MHz, DMSO-*d*₆, δ ppm): 12.56 (s, 1H), 10.85 (s, 1H), 7.92 (d, *J* = 8.6 Hz, 2H), 7.75 (d, *J* = 7.9 Hz, 1H), 7.70 (s, 1H), 7.50 (d, *J* = 8.6 Hz, 2H), 7.33 (d, *J* = 8.0 Hz, 1H), 7.21 (d, *J* = 1.7 Hz, 1H), 7.16 (d, *J* = 7.6 Hz, 1H), 7.06 (t, *J* = 7.2 Hz, 1H), 6.98 (t, *J* = 7.3 Hz, 1H), 4.51 (q, *J* = 8.3 Hz, 1H), 3.15 (dd, *J* = 5.3, 14.4 Hz, 1H), 3.00 (dd, *J* = 9.5, 14.2 Hz, 1H), 1.32 (s, 9H). ¹³C-NMR (100 MHz, DMSO-*d*₆, δ ppm): 171.8, 158.0, 155.2, 147.6, 135.9, 133.1, 132.2, 128.7, 127.3, 127.1, 124.1, 120.8, 118.7, 118.1, 111.2, 109.4, 108.8, 78.2, 55.0, 28.1, 27.4. HR-ESI-MS (*m/z*): [M + H]⁺ calcd for C₂₅H₂₆ClN₄O₃S, 497.1409; found, 497.1383.

4.26. *tert*-Butyl (S)-(1-((4-(4-chlorophenyl)thiazol-2-yl)amino)-3,3-dimethyl-1-oxobutan-2-yl)carbamate (5l)

White solid. Yield: 154 mg (36%). Mp 124–126 °C. FT-IR (KBr) ν_{\max} (cm⁻¹): 3426, 3339, 3251, 3090, 2969, 1677, 1550, 1512, 1367, 1246, 1162, 1055, 844, 742, 551. ¹H-NMR (600 MHz, DMSO-*d*₆, δ ppm): 12.30 (s, 1H), 7.92 (dd, *J* = 1.8, 7.2 Hz, 2H), 7.69 (s, 1H), 7.49 (dd, *J* = 1.8, 6.9 Hz, 2H), 6.93 (d, *J* = 7.8 Hz, 1H), 4.20 (d, *J* = 7.8 Hz, 1H), 1.39 (s, 9H), 0.97 (s, 9H). ¹³C-NMR (150 MHz, DMSO-*d*₆, δ ppm): 170.3, 157.6, 155.5, 147.7, 133.1, 132.3, 128.7, 127.4, 108.9, 78.4, 62.1, 34.0, 28.1, 26.4. HR-ESI-MS (*m/z*): [M + H]⁺ calcd for C₂₀H₂₇ClN₃O₃S, 424.1456; found, 424.1463.

4.27. *tert*-Butyl (S)-(1-((4-(4-fluorophenyl)thiazol-2-yl)amino)-1-oxo-3-phenylpropan-2-yl)carbamate (5m)

White solid. Yield: 247 mg (56%). Mp 197–199 °C. FT-IR (KBr) ν_{\max} (cm⁻¹): 3381, 3356, 2977, 1694, 1545, 1447, 1320, 1274, 1165, 1056, 848, 740, 699. ¹H-NMR (400 MHz, DMSO-*d*₆, δ ppm): 12.52 (s, 1H), 7.95 (dd, *J* = 5.5, 8.7 Hz, 2H), 7.63 (s, 1H), 7.37 (d, *J* = 7.1 Hz, 2H), 7.32–7.25 (m, 5H), 7.21 (t, *J* = 7.2 Hz, 1H), 4.50–4.44 (m, 1H), 3.04 (dd, *J* = 4.2, 13.6 Hz, 1H), 2.83 (dd, *J* = 10.7, 13.5 Hz, 1H), 1.32 (s, 9H). ¹³C-NMR (100 MHz, DMSO-*d*₆, δ ppm): 171.3, 162.9, 160.5, 157.8, 155.4, 147.8, 137.6, 130.8, 130.8, 129.3, 128.0, 127.6, 127.6, 126.3, 115.7, 115.4, 107.9, 78.2, 55.9, 36.8, 28.0. HR-ESI-MS (*m/z*): [M + H]⁺ calcd for C₂₃H₂₅FN₃O₃S, 442.1595; found, 442.1589.

4.28. *tert*-Butyl (S)-(1-((4-(4-fluorophenyl)thiazol-2-yl)amino)-3-(1*H*-indol-3-yl)-1-oxopropan-2-yl)carbamate (5n)

White solid. Yield: 205 mg (43%). Mp 200–202 °C. FT-IR (KBr) ν_{\max} (cm⁻¹): 3390, 3346, 3060, 2977, 2928, 1691, 1545, 1366, 1261, 1238, 1164, 1058, 844, 743, 513. ¹H-NMR (400 MHz, DMSO-*d*₆, δ ppm): 12.54 (s, 1H), 10.85 (s, 1H), 7.96–7.93 (m, 2H), 7.75 (d, *J* = 8.0 Hz, 1H), 7.62 (s, 1H), 7.34–7.24 (m, 3H), 7.21 (d, *J* = 1.8 Hz, 1H), 7.15 (d, *J* = 7.7 Hz, 1H), 7.06 (t, *J* = 7.1 Hz, 1H), 6.98 (t, *J* = 7.4 Hz, 1H), 4.52 (q, *J* = 8.3 Hz, 1H), 3.15 (dd, *J* = 5.3, 14.3 Hz, 1H), 3.00 (dd, *J* = 9.5, 14.4 Hz, 1H), 1.32 (s, 9H). ¹³C-NMR (100 MHz, DMSO-*d*₆, δ ppm): 171.8, 162.9, 160.5, 157.9, 155.2, 147.8, 135.9, 130.9, 130.8, 127.6, 127.6, 127.1, 124.1, 120.8, 118.7, 118.1, 115.6, 115.4, 111.2, 109.4, 107.9, 78.2, 55.0, 28.1, 27.4. HR-ESI-TOF-MS (*m/z*): [M + H]⁺ calcd for C₂₅H₂₆FN₄O₃S, 481.1710; found, 481.1713.

4.29. *tert*-Butyl (S)-(1-((4-(4-fluorophenyl)thiazol-2-yl)amino)-3-methyl-1-oxobutan-2-yl)carbamate (5o)

White solid. Yield: 150 mg (38%). Mp 195–197 °C. FT-IR (KBr) ν_{\max} (cm⁻¹): 3290, 3073, 2975, 2876, 1668, 1548, 1374, 1280, 1163, 993, 844, 738, 512. ¹H-NMR (400 MHz, DMSO-*d*₆, δ ppm): 12.31 (s, 1H), 7.94 (dd, *J* = 5.6, 8.8 Hz, 2H), 7.61 (s, 1H), 7.27 (t, *J* = 8.9 Hz, 2H), 7.11 (d, *J* = 8.2 Hz, 1H), 4.08 (t, *J* = 7.9 Hz, 1H), 2.04–1.99 (m, 1H), 1.39 (s, 9H), 0.89 (t, *J* = 6.3 Hz, 6H). ¹³C-NMR (100 MHz, DMSO-*d*₆, δ ppm): 171.2, 155.5, 147.8, 130.8, 127.6, 115.6, 115.4, 107.8, 78.2, 59.7, 29.9, 28.1, 18.9, 18.4. HR-ESI-MS (*m/z*): [M + H]⁺ calcd for C₁₉H₂₅FN₃O₃S, 394.1595; found, 394.1602.

4.30. *tert*-Butyl (S)-(1-oxo-3-phenyl-1-((4-(4-(trifluoromethyl)phenyl)thiazol-2-yl)amino)propan-2-yl)carbamate (5p)

White solid. Yield: 119 mg (24%). Mp 109–111 °C. FT-IR (KBr) ν_{\max} (cm⁻¹): 3300, 3192, 3065, 2980, 2935, 1664, 1555, 1321, 1165, 1119, 1065, 849, 749, 707. ¹H-NMR (400 MHz, DMSO-*d*₆, δ ppm): 12.61 (s, 1H), 8.13 (d, *J* = 8.2 Hz, 2H), 7.89 (s, 1H), 7.81 (d, *J* = 8.4 Hz, 2H), 7.38 (d, *J* = 7.2 Hz, 2H), 7.34–7.28 (m, 3H), 7.21 (t, *J* = 7.2 Hz, 1H), 4.51–4.45 (m, 1H), 3.05 (dd, *J* = 4.2, 13.6 Hz, 1H), 2.83 (dd, *J* = 10.8, 13.4 Hz, 1H), 1.32 (s, 9H). ¹³C-NMR (100 MHz, DMSO-*d*₆, δ ppm): 171.5, 158.1, 155.4, 147.3, 137.9, 137.6, 129.3, 128.0, 126.4, 126.2, 125.7, 110.8, 78.2, 56.0,



36.8, 28.0. HR-ESI-MS (m/z): $[M + H]^+$ calcd for $C_{24}H_{25}F_3N_3O_3S$, 492.1563; found, 492.1513.

4.31. *tert*-Butyl (S)-(3-(1*H*-indol-3-yl)-1-oxo-1-((4-(trifluoromethyl)phenyl)thiazol-2-yl)amino)propan-2-yl carbamate (5q)

White solid. Yield: 108 mg (20%). Mp 125–127 °C. FT-IR (KBr) ν_{\max} (cm^{-1}): 3493, 3310, 3059, 2978, 1686, 1665, 1546, 1322, 1165, 1119, 1065, 847, 744. 1H -NMR (400 MHz, DMSO- d_6 , δ ppm): 12.63 (s, 1H), 10.85 (s, 1H), 8.12 (d, $J = 8.1$ Hz, 2H), 7.88 (s, 1H), 7.81 (d, $J = 8.3$ Hz, 2H), 7.75 (d, $J = 8.0$ Hz, 1H), 7.33 (d, $J = 8.0$ Hz, 1H), 7.21 (d, $J = 1.8$ Hz, 1H), 7.17 (d, $J = 7.5$ Hz, 1H), 7.06 (t, $J = 7.2$ Hz, 1H), 6.98 (t, $J = 7.3$ Hz, 1H), 4.52 (q, $J = 8.4$ Hz, 1H), 3.16 (dd, $J = 5.2, 14.4$ Hz, 1H), 3.01 (dd, $J = 9.5, 14.3$ Hz, 1H), 1.33 (s, 9H). ^{13}C -NMR (100 MHz, DMSO- d_6 , δ ppm): 171.9, 158.2, 155.3, 147.2, 137.9, 135.9, 127.1, 126.2, 125.7, 124.1, 122.9, 120.8, 118.7, 118.1, 111.2, 110.7, 109.4, 78.2, 55.1, 28.1, 27.4. HR-ESI-MS (m/z): $[M + H]^+$ calcd for $C_{26}H_{26}F_3N_4O_3S$, 531.1672; found, 531.1678.

4.32. *tert*-Butyl (S)-(3,3-dimethyl-1-oxo-1-((4-(trifluoromethyl)phenyl)thiazol-2-yl)amino)butan-2-yl carbamate (5r)

White solid. Yield: 157 mg (34%). Mp 181–183 °C. FT-IR (KBr) ν_{\max} (cm^{-1}): 3447, 3341, 3210, 3077, 2973, 1669, 1619, 1549, 1372, 1324, 1270, 1167, 1065, 851, 714. 1H -NMR (600 MHz, DMSO- d_6 , δ ppm): 12.37 (s, 1H), 8.12 (d, $J = 8.4$ Hz, 2H), 7.86 (s, 1H), 7.80 (d, $J = 8.4$ Hz, 2H), 6.95 (d, $J = 7.2$ Hz, 1H), 4.21 (d, $J = 7.8$ Hz, 1H), 1.39 (s, 9H), 0.97 (s, 9H). ^{13}C -NMR (150 MHz, DMSO- d_6 , δ ppm): 170.4, 157.8, 155.5, 147.4, 138.0, 128.0, 127.8, 126.3, 125.7, 125.7, 125.2, 123.4, 110.8, 78.4, 62.1, 33.9, 28.1, 26.4. HR-ESI-MS (m/z): $[M + H]^+$ calcd for $C_{21}H_{27}F_3N_3O_3S$, 458.1720; found, 458.1728.

4.33. *tert*-Butyl (S)-(1-((4-(2,4-dihydroxyphenyl)thiazol-2-yl)amino)-1-oxo-3-phenylpropan-2-yl)carbamate (5s)

White solid. Yield: 130 mg (29%). Mp 140–142 °C. FT-IR (KBr) ν_{\max} (cm^{-1}): 3609, 3532, 3327, 3256, 2981, 1672, 1630, 1541, 1453, 1368, 1284, 1162, 1048, 852, 704. 1H -NMR (400 MHz, DMSO- d_6 , δ ppm): 12.46 (s, 1H), 10.81 (s, 1H), 9.53 (s, 1H), 7.69 (d, $J = 8.4$ Hz, 1H), 7.46 (s, 1H), 7.35 (t, $J = 5.8$ Hz, 3H), 7.29 (t, $J = 7.5$ Hz, 2H), 7.21 (t, $J = 7.2$ Hz, 1H), 6.35 (d, $J = 2.3$ Hz, 1H), 6.32 (dd, $J = 2.4, 8.5$ Hz, 1H), 4.48–4.42 (m, 1H), 3.04 (dd, $J = 4.3, 13.6$ Hz, 1H), 2.84 (dd, $J = 10.6, 13.5$ Hz, 1H), 1.32 (s, 9H). ^{13}C -NMR (100 MHz, DMSO- d_6 , δ ppm): 171.1, 158.3, 156.6, 156.3, 155.4, 146.6, 137.6, 129.2, 128.4, 128.0, 126.4, 110.8, 107.1, 105.8, 102.9, 78.3, 55.9, 36.8, 28.1. HR-ESI-MS (m/z): $[M + H]^+$ calcd for $C_{23}H_{26}N_3O_5S$, 456.1588; found, 456.1560.

4.34. *tert*-Butyl (S)-(1-((4-(2,4-dihydroxyphenyl)thiazol-2-yl)amino)-3-(1*H*-indol-3-yl)-1-oxopropan-2-yl)carbamate (5t)

White solid. Yield: 105 mg (21%). Mp 193–195 °C. FT-IR (KBr) ν_{\max} (cm^{-1}): 3357, 3112, 3053, 2974, 1670, 1631, 1558, 1525, 1449, 1320, 1164, 1050, 845, 743, 700. 1H -NMR (400 MHz, DMSO- d_6 , δ ppm): 12.47 (s, 1H), 10.85 (s, 2H), 9.52 (s, 1H), 7.70

(dd, $J = 8.3, 10.5$ Hz, 2H), 7.45 (s, 1H), 7.33 (d, $J = 8.0$ Hz, 1H), 7.21–7.19 (m, 2H), 7.06 (t, $J = 7.2$ Hz, 1H), 6.98 (t, $J = 7.3$ Hz, 1H), 6.34–6.30 (m, 2H), 4.50 (q, $J = 8.1$ Hz, 1H), 3.16 (dd, $J = 5.4, 14.4$ Hz, 1H), 3.01 (dd, $J = 9.3, 14.4$ Hz, 1H), 1.33 (s, 9H). ^{13}C -NMR (100 MHz, DMSO- d_6 , δ ppm): 171.5, 158.3, 156.7, 156.4, 155.3, 146.6, 135.9, 128.3, 127.1, 124.0, 120.9, 118.6, 118.2, 111.2, 110.7, 109.4, 107.1, 105.7, 102.9, 78.2, 55.1, 28.1, 27.3. HR-ESI-MS (m/z): $[M + H]^+$ calcd for $C_{25}H_{27}N_4O_5S$, 495.1697; found, 495.1706.

4.35. *tert*-Butyl (S)-(1-((4-(1*H*-benzo[*d*]imidazole-2-yl)thiazol-2-yl)amino)-1-oxo-3-phenylpropan-2-yl)carbamate (5u)

White solid. Yield: 220 mg (47%). Mp 211–213 °C. FT-IR (KBr) ν_{\max} (cm^{-1}): 3444, 3322, 3191, 3069, 2974, 2931, 2811, 2719, 1718, 1667, 1551, 1490, 1401, 1262, 1164, 1020, 851, 745, 701. 1H -NMR (400 MHz, DMSO- d_6 , δ ppm): 12.63 (s, 1H), 12.52 (s, 1H), 7.92 (s, 1H), 7.59 (s, 2H), 7.37 (d, $J = 7.2$ Hz, 3H), 7.30 (t, $J = 7.5$ Hz, 2H), 7.21 (dt, $J = 3.8, 6.2$ Hz, 3H), 4.56 (td, $J = 4.7, 10.3$ Hz, 1H), 3.06 (dd, $J = 4.5, 13.6$ Hz, 1H), 2.87 (dd, $J = 10.5, 13.5$ Hz, 1H), 1.33 (s, 9H). ^{13}C -NMR (100 MHz, DMSO- d_6 , δ ppm): 171.6, 158.1, 155.4, 147.1, 141.0, 137.5, 129.2, 128.1, 126.4, 121.7, 113.4, 78.3, 55.8, 36.8, 28.0. HR-ESI-MS (m/z): $[M + H]^+$ calcd for $C_{24}H_{26}N_5O_3S$, 464.1751; found, 464.1749.

4.36. *tert*-Butyl (S)-(1-((4-(1*H*-benzo[*d*]imidazole-2-yl)thiazol-2-yl)amino)-3-(1*H*-indol-3-yl)-1-oxopropan-2-yl)carbamate (5v)

White solid. Yield: 260 mg (52%). Mp 153–155 °C. FT-IR (KBr) ν_{\max} (cm^{-1}): 3191, 3059, 2972, 1687, 1547, 1500, 1364, 1276, 1162, 1051, 847, 742. 1H -NMR (400 MHz, DMSO- d_6 , δ ppm): 12.63 (s, 1H), 12.54 (s, 1H), 10.86 (s, 1H), 7.91 (s, 1H), 7.72 (d, $J = 7.9$ Hz, 1H), 7.58 (s, 2H), 7.33 (d, $J = 8.0$ Hz, 1H), 7.23–7.19 (m, 4H), 7.06 (t, $J = 6.9$ Hz, 1H), 6.98 (t, $J = 7.3$ Hz, 1H), 4.60 (td, $J = 5.7, 8.2$ Hz, 1H), 3.18 (dd, $J = 5.6, 14.5$ Hz, 1H), 3.04 (dd, $J = 9.2, 14.5$ Hz, 1H), 1.34 (s, 9H). ^{13}C -NMR (100 MHz, DMSO- d_6 , δ ppm): 172.0, 158.2, 155.3, 147.2, 141.0, 135.9, 127.1, 124.0, 120.8, 118.6, 118.2, 113.4, 111.2, 109.4, 78.3, 55.0, 28.1, 27.4. HR-ESI-MS (m/z): $[M + H]^+$ calcd for $C_{26}H_{27}N_6O_3S$, 503.1860; found, 503.1860.

4.37. *tert*-Butyl (S)-(1-((4-(furan-2-yl)thiazol-2-yl)amino)-1-oxo-3-phenylpropan-2-yl)carbamate (5w)

White solid. Yield: 101 mg (24%). Mp 192–194 °C. FT-IR (KBr) ν_{\max} (cm^{-1}): 3281, 3063, 2979, 2934, 1706, 1659, 1550, 1446, 1374, 1291, 1166, 1014, 855, 740. 1H -NMR (400 MHz, DMSO- d_6 , δ ppm): 12.60 (s, 1H), 7.73 (s, 1H), 7.35 (d, $J = 9.7$ Hz, 3H), 7.28 (t, $J = 7.4$ Hz, 3H), 7.20 (t, $J = 7.1$ Hz, 1H), 6.68 (d, $J = 3.0$ Hz, 1H), 6.59 (s, 1H), 4.43–4.40 (m, 1H), 3.02 (dd, $J = 3.8, 13.5$ Hz, 1H), 2.84–2.78 (m, 1H), 1.30 (s, 9H). ^{13}C -NMR (100 MHz, DMSO- d_6 , δ ppm): 171.5, 155.5, 150.0, 142.9, 140.9, 137.7, 129.4, 128.1, 126.5, 111.8, 107.2, 106.5, 78.3, 56.1, 36.9, 28.2. HR-ESI-MS (m/z): $[M + Na]^+$ calcd for $C_{21}H_{23}N_3NaO_4S$, 436.1301; found, 436.1396.



4.38. *tert*-Butyl (S)-(1-((4-(furan-2-yl)thiazol-2-yl)amino)-3-(1*H*-indol-3-yl)-1-oxopropan-2-yl)carbamate (5x)

White solid. Yield: 91 mg (20%). Mp 180–182 °C. FT-IR (KBr) ν_{\max} (cm⁻¹): 3457, 3286, 3057, 2974, 1686, 1544, 1451, 1364, 1289, 1163, 1067, 1016, 815, 741. ¹H-NMR (400 MHz, DMSO-*d*₆, δ ppm): 12.63 (s, 1H), 10.84 (s, 1H), 7.75–7.73 (m, 2H), 7.33 (d, *J* = 10.2 Hz, 2H), 7.20–7.19 (m, 1H), 7.13 (d, *J* = 7.6 Hz, 1H), 7.06 (t, *J* = 7.4 Hz, 1H), 6.97 (t, *J* = 7.4 Hz, 1H), 6.68 (d, *J* = 3.1 Hz, 1H), 6.59 (dd, *J* = 1.8, 3.3 Hz, 1H), 4.48 (q, *J* = 8.4 Hz, 1H), 3.14 (dd, *J* = 5.2, 14.3 Hz, 1H), 2.99 (dd, *J* = 9.5, 14.3 Hz, 1H), 1.32 (s, 9H). ¹³C-NMR (100 MHz, DMSO-*d*₆, δ ppm): 171.8, 158.3, 155.2, 149.9, 142.8, 140.8, 135.9, 127.1, 124.1, 120.8, 118.7, 118.1, 111.7, 111.2, 109.4, 107.0, 106.3, 78.2, 55.1, 28.1, 27.4. HR-ESI-MS (*m/z*): [M + H]⁺ calcd for C₂₃H₂₅N₄O₄S, 453.1591; found, 453.1588.

4.39. *tert*-Butyl (S)-(1-oxo-3-phenyl-1-((4-(thiophen-2-yl)thiazol-2-yl)amino)propan-2-yl)carbamate (5y)

White solid. Yield: 136 mg (32%). Mp 168–170 °C. FT-IR (KBr) ν_{\max} (cm⁻¹): 3288, 3185, 3061, 2976, 2932, 1659, 1543, 1370, 1286, 1166, 1050, 851, 695. ¹H-NMR (400 MHz, DMSO-*d*₆, δ ppm): 12.60 (s, 1H), 7.53 (dd, *J* = 1.1, 3.5 Hz, 1H), 7.51–7.48 (m, 2H), 7.37 (d, *J* = 7.2 Hz, 2H), 7.29 (t, *J* = 7.6 Hz, 3H), 7.21 (t, *J* = 7.3 Hz, 1H), 7.11 (dd, *J* = 3.5, 5.1 Hz, 1H), 4.48–4.42 (m, 1H), 3.03 (dd, *J* = 4.1, 13.5 Hz, 1H), 2.81 (dd, *J* = 10.8, 13.4 Hz, 1H), 1.31 (s, 9H). ¹³C-NMR (100 MHz, DMSO-*d*₆, δ ppm): 171.4, 157.7, 155.4, 143.7, 138.3, 137.6, 129.3, 128.0, 126.3, 125.5, 123.7, 106.5, 78.2, 55.9, 36.8, 28.0, 27.7. HR-ESI-TOF-MS (*m/z*): [M + Na]⁺ calcd for C₂₁H₂₃N₃O₃S₂Na, 452.1079; found, 452.1074.

4.40. *tert*-Butyl (S)-(3-(1*H*-indol-3-yl)-1-oxo-1-((4-(thiophen-2-yl)thiazol-2-yl)amino)propan-2-yl)carbamate (5z)

White solid. Yield: 220 mg (47%). Mp 185–187 °C. FT-IR (KBr) ν_{\max} (cm⁻¹): 3461, 3302, 3182, 3057, 2975, 1658, 1536, 1362, 1290, 1165, 1052, 847, 801, 740, 708. ¹H-NMR (400 MHz, DMSO-*d*₆, δ ppm): 12.62 (s, 1H), 10.85 (s, 1H), 7.75 (d, *J* = 8.0 Hz, 1H), 7.53–7.47 (m, 3H), 7.32 (d, *J* = 8.1 Hz, 1H), 7.20 (d, *J* = 1.8 Hz, 1H), 7.14 (d, *J* = 7.5 Hz, 1H), 7.11 (dd, *J* = 3.5, 5.1 Hz, 1H), 7.06 (t, *J* = 7.4 Hz, 1H), 6.98 (t, *J* = 7.3 Hz, 1H), 4.50 (q, *J* = 8.4 Hz, 1H), 3.14 (dd, *J* = 5.3, 14.3 Hz, 1H), 2.99 (dd, *J* = 9.6, 14.3 Hz, 1H), 1.32 (s, 9H). ¹³C-NMR (100 MHz, DMSO-*d*₆, δ ppm): 171.8, 157.8, 155.2, 143.6, 138.3, 135.9, 128.0, 127.1, 125.4, 124.1, 123.7, 120.8, 118.7, 118.1, 111.2, 109.4, 106.4, 78.2, 55.0, 36.1, 28.1. HR-ESI-TOF-MS (*m/z*): [M + H]⁺ calcd for C₂₃H₂₅N₄O₃S₂, 469.1368; found, 469.1363.

4.41. *tert*-Butyl (S)-(1-oxo-3-phenyl-1-((4-(thiophen-3-yl)thiazol-2-yl)amino)propan-2-yl)carbamate (5aa)

White solid. Yield: 166 mg (39%). Mp 205–207 °C. FT-IR (KBr) ν_{\max} (cm⁻¹): 3354, 3282, 3104, 3060, 2975, 2932, 1694, 1546, 1449, 1373, 1276, 1160, 1037, 954, 847, 796, 727, 604. ¹H-NMR (400 MHz, DMSO-*d*₆, δ ppm): 12.53 (s, 1H), 7.79 (dd, *J* = 1.1, 2.8 Hz, 1H), 7.62 (dd, *J* = 3.0, 5.0 Hz, 1H), 7.57 (dd, *J* = 1.2, 5.0 Hz, 1H), 7.48 (s, 1H), 7.37 (d, *J* = 7.2 Hz, 2H), 7.29 (t, *J* = 7.4 Hz, 3H), 7.20 (t, *J* = 7.2 Hz, 1H), 4.46 (td, *J* = 4.3, 9.5 Hz, 1H),

3.04 (dd, *J* = 4.2, 13.6 Hz, 1H), 2.82 (dd, *J* = 10.8, 13.4 Hz, 1H), 1.31 (s, 9H). ¹³C-NMR (100 MHz, DMSO-*d*₆, δ ppm): 171.3, 157.6, 155.4, 145.3, 137.6, 136.6, 129.3, 128.0, 127.0, 126.3, 125.9, 121.4, 107.6, 78.2, 55.9, 36.9, 28.0. HR-ESI-MS (*m/z*): [M + H]⁺ calcd for C₂₁H₂₄N₃O₃S₂, 430.1254; found, 430.1231.

4.42. *tert*-Butyl (S)-(3-(1*H*-indol-3-yl)-1-oxo-1-((4-(thiophen-3-yl)thiazol-2-yl)amino)propan-2-yl)carbamate (5ab)

White solid. Yield: 98 mg (21%). Mp 136–138 °C. FT-IR (KBr) ν_{\max} (cm⁻¹): 3469, 3281, 3190, 3062, 2971, 1688, 1547, 1366, 1295, 1165, 1057, 843, 734. ¹H-NMR (400 MHz, DMSO-*d*₆, δ ppm): 12.55 (s, 1H), 10.84 (s, 1H), 7.78–7.74 (m, 2H), 7.61 (dd, *J* = 3.0, 5.0 Hz, 1H), 7.57 (dd, *J* = 1.2, 5.0 Hz, 1H), 7.47 (s, 1H), 7.32 (d, *J* = 8.0 Hz, 1H), 7.20 (d, *J* = 1.8 Hz, 1H), 7.13 (d, *J* = 7.6 Hz, 1H), 7.06 (t, *J* = 7.4 Hz, 1H), 6.98 (t, *J* = 7.4 Hz, 1H), 4.53–4.47 (m, 1H), 3.15 (dd, *J* = 5.2, 14.3 Hz, 1H), 3.00 (dd, *J* = 9.6, 14.3 Hz, 1H), 1.32 (s, 9H). ¹³C-NMR (100 MHz, DMSO-*d*₆, δ ppm): 171.8, 157.8, 155.3, 145.4, 136.7, 136.0, 127.2, 127.1, 126.1, 124.2, 121.4, 120.9, 118.9, 118.2, 111.3, 109.5, 107.7, 78.3, 55.1, 28.2, 27.5. HR-ESI-TOF-MS (*m/z*): [M + H]⁺ calcd for C₂₃H₂₅N₄O₃S₂, 469.1366; found, 469.1366.

4.43. *tert*-Butyl (S)-(1-oxo-3-phenyl-1-((4-(pyridin-2-yl)thiazol-2-yl)amino)propan-2-yl)carbamate (5ac)

White solid. Yield: 150 mg (35%). Mp 90–92 °C. FT-IR (KBr) ν_{\max} (cm⁻¹): 3199, 3062, 2974, 1675, 1552, 1451, 1371, 1277, 1165, 1052, 851, 747, 698. ¹H-NMR (400 MHz, DMSO-*d*₆, δ ppm): 12.57 (s, 1H), 8.62 (ddd, *J* = 0.9, 1.7, 4.8 Hz, 1H), 7.96 (d, *J* = 7.8 Hz, 1H), 7.90 (td, *J* = 1.7, 7.7 Hz, 1H), 7.85 (s, 1H), 7.39–7.28 (m, 6H), 7.21 (t, *J* = 7.3 Hz, 1H), 4.51–4.45 (m, 1H), 3.05 (dd, *J* = 4.1, 13.6 Hz, 1H), 2.83 (dd, *J* = 10.8, 13.4 Hz, 1H), 1.32 (s, 9H). ¹³C-NMR (100 MHz, DMSO-*d*₆, δ ppm): 171.4, 158.0, 155.4, 151.9, 149.5, 149.1, 137.6, 137.3, 129.3, 128.0, 126.3, 122.8, 119.9, 111.7, 78.2, 55.9, 36.8, 28.0. HR-ESI-MS (*m/z*): [M + H]⁺ calcd for C₂₂H₂₅N₄O₃S, 425.1642; found, 425.1652.

4.44. *tert*-Butyl (S)-(3-(1*H*-indol-3-yl)-1-oxo-1-((4-(pyridin-2-yl)thiazol-2-yl)amino)propan-2-yl)carbamate (5ad)

White solid. Yield: 140 mg (30%). Mp 204–206 °C. FT-IR (KBr) ν_{\max} (cm⁻¹): 3351, 3226, 3055, 2974, 1722, 1684, 1551, 1519, 1425, 1345, 1282, 1240, 1161, 1001, 855, 749, 665. ¹H-NMR (400 MHz, DMSO-*d*₆, δ ppm): 12.59 (s, 1H), 10.85 (s, 1H), 8.61 (ddd, *J* = 0.9, 1.7, 4.8 Hz, 1H), 7.95 (d, *J* = 7.8 Hz, 1H), 7.89 (td, *J* = 1.8, 7.7 Hz, 1H), 7.84 (s, 1H), 7.76 (d, *J* = 7.8 Hz, 1H), 7.36–7.32 (m, 2H), 7.22 (d, *J* = 1.8 Hz, 1H), 7.16 (d, *J* = 7.5 Hz, 1H), 7.06 (t, *J* = 7.1 Hz, 1H), 6.98 (t, *J* = 7.3 Hz, 1H), 4.53 (q, *J* = 8.4 Hz, 1H), 3.17 (dd, *J* = 5.3, 14.3 Hz, 1H), 3.01 (dd, *J* = 9.4, 14.3 Hz, 1H), 1.33 (s, 9H). ¹³C-NMR (100 MHz, DMSO-*d*₆, δ ppm): 171.8, 158.1, 155.3, 151.9, 149.5, 149.0, 137.3, 135.9, 127.1, 124.1, 122.8, 120.8, 119.9, 118.7, 118.1, 111.7, 111.2, 109.4, 78.2, 55.0, 28.1, 27.4. HR-ESI-MS (*m/z*): [M + H]⁺ calcd for C₂₄H₂₆N₅O₃S, 464.1751; found, 464.1758.



4.45 Cytotoxicity assay

The cytotoxic activities of the synthesized compounds were evaluated against three human cancer cell lines (A549, HeLa, and MCF-7) using the MTT assay with specific modifications as described.⁵² A549 (RCB3677), HeLa (RCB3680), and MCF7 (RCB1904) cell lines were purchased from the RIKEN Cell Bank. All synthesized compounds were dissolved in DMSO to make 10 mM stock solutions. Serial dilutions were prepared in the culture medium. The positive control, 5-FU, was dissolved in DMSO to make a 10 mM stock solution and then stored at -20°C until use.

The human cancer cell lines were cultured in α -minimum essential medium (α -MEM), supplemented with 1% antibiotic antimycotic solution and 10% fetal bovine serum, at 37°C and in 5% CO_2 atmosphere. Cells at 80–90% confluency were harvested and centrifuged at 3000 rpm for 3 min. The supernatant was discarded and the cell pellet was resuspended in fresh medium. Aliquots (100 μL) of the cells were seeded in 96-well plates (1×10^4 cells per well) and incubated for 24 hours. The cells were then washed with phosphate-buffered saline (PBS), and five concentrations of tested compounds (6.25, 12.5, 25, 50, 100 μM), including the positive control, 5-FU, were added to the wells. After a 72 hours incubation, the cells were washed with PBS, and 100 μL aliquots of medium containing MTT solution (5 mg mL^{-1}) were added to each well and incubated for 3 hours. The absorbance was recorded using a microplate reader at 570 nm. Percent proliferation inhibition was calculated using the following formula:

$$\% \text{ Proliferation cell inhibition} = [(A_t - A_b)/(A_c - A_b)] \times 100$$

A_t : absorbance of test compound, A_b : absorbance of blank, A_c : absorbance of control.

The concentrations (IC_{50} values) of the compounds required to inhibit 50% of the growth of the human cancer cell lines were calculated based on the relationship between the concentrations and the percentage of inhibition, using the GraphPad Prism 5.0 software. Each experiment was performed three times, and all data are presented as mean \pm standard deviation (S.D.).

Data availability

The data supporting this article have been included as part of the ESI.†

Author contributions

Hieu Trong Le: investigation, writing original draft. Nguyen Thi Huong Nguyen: investigation. Quang Vinh Hong: investigation. Zhuang Qian: investigation. Thi Minh Bui: investigation. Linh Nhut Huynh: investigation. Saw Yu Yu Hnin: investigation. Zin Paing Htoo: investigation. An Pham Thuy Le: investigation. De Quang Tran: investigation. Hiroyuki Morita: review & editing, supervision. Hue Thi Buu Bui: writing – review & editing, visualization, supervision, conceptualization. All authors gave final

approval for publication and agreed to be held accountable for the work performed therein.

Conflicts of interest

There are no conflicts to declare.

Acknowledgements

Hieu Trong Le was funded by the Master, PhD Scholarship Programme of Vingroup Innovation Foundation (VINIF), code VINIF.2024.TS.029. This work was supported in part by a Grant-in-Aid for Scientific Research from the Ministry of Education, Culture, Sports, Science and Technology, Japan (JSPS KAKENHI Grant JP 25K02418 to H. M.).

References

- (a) C. V. Junior, A. Danuello, V. da S. Bolzani, E. J. Barreiro and C. A. Fraga, *Curr. Med. Chem.*, 2007, **14**, 1829–1852; (b) S. M. Shaveta and P. Singh, *Eur. J. Med. Chem.*, 2016, **124**, 500–536; (c) G. Bérubé, *Expet Opin. Drug Discov.*, 2016, **11**, 281–305; (d) G. Teli and P. A. Chawla, *ChemistrySelect*, 2021, **6**, 4803–4836.
- Z. Zeng, C. Liao and L. Yu, *Chin. Chem. Lett.*, 2024, **35**, 109349.
- Y. Q. Meng, J. Ren, J. X. Sun, *et al.*, *Eur. J. Med. Chem.*, 2024, **269**, 116311.
- R. G. Vaswani, D. S. Huang, N. Anthony, *et al.*, *J. Med. Chem.*, 2025, **68**, 1772–1792.
- J. B. Chen, T. R. Chern, T. T. Wei, C. C. Chen, J. H. Lin and J. M. Fang, *J. Med. Chem.*, 2013, **56**, 3645–3655.
- C. J. Lai, R. Bao, X. U. Tao, *et al.*, *Cancer Res.*, 2010, **70**, 3647–3656.
- C. Qian, C. J. Lai, R. Bao, *et al.*, *Clin. Cancer Res.*, 2012, **18**, 4104–4113.
- K. S. Ko, M. E. Steffey, K. R. Brandvold and M. B. Soellner, *ACS Med. Chem. Lett.*, 2013, **4**, 779–783.
- G. Wu, *Amino Acids*, 2009, **37**, 1–17.
- Y. N. Zhang, W. Zhang, D. Hong, *et al.*, *Bioorg. Med. Chem.*, 2008, **16**, 8697–8705.
- V. Anbharasi, N. Cao and S. S. Feng, *J. Biomed. Mater. Res., Part A*, 2010, **94**, 730–743.
- M. K. Kim, K. S. Park, W. S. Yeo, H. Choo and Y. Chong, *Bioorg. Med. Chem.*, 2009, **17**, 1164–1171.
- S. R. Alizadeh and S. M. Hashemi, *Med. Chem. Res.*, 2021, **30**, 771–806.
- A. F. Kassem, R. H. Althomali, M. M. Anwar and W. I. El-Sofany, *J. Mol. Struct.*, 2024, **1303**, 137510.
- S. Bathula, M. Sankaranarayanan, B. Malgija, I. Kaliappan, R. R. Bhandare and A. B. Shaik, *ACS Omega*, 2023, **8**, 44287–44311.
- A. Ayati, S. Emami, S. Moghimi and A. Foroumadi, *Future Med. Chem.*, 2019, **11**, 1929–1952.
- P. Furet, V. Guagnano, R. A. Fairhurst, *et al.*, *Bioorg. Med. Chem. Lett.*, 2013, **23**, 3741–3748.



- 18 L. J. Lombardo, F. Y. Lee, P. Chen, *et al.*, *J. Med. Chem.*, 2004, **47**, 6658–6661.
- 19 A. M. Menzies, G. V. Long and R. Murali, *Drug Des. Dev. Ther.*, 2012, **6**, 391–405.
- 20 S. Goodin, M. P. Kane and E. H. Rubin, *J. Clin. Oncol.*, 2004, **22**, 2015–2025.
- 21 M. Lopus, G. Smiyun, H. Miller, E. Oroudjev, L. Wilson and M. A. Jordan, *Cancer Chemother. Pharmacol.*, 2015, **76**, 1013–1024.
- 22 M. Kriek, F. Martins, R. Leonardi, S. A. Fairhurst, D. J. Lowe and P. L. Roach, *J. Biol. Chem.*, 2007, **282**, 17413–17423.
- 23 S. Kumari, A. V. Carmona, A. K. Tiwari and P. C. Trippier, *J. Med. Chem.*, 2020, **63**, 12290–12358.
- 24 J. Hong and H. Luesch, *Nat. Prod. Rep.*, 2012, **29**, 449.
- 25 J. Herrmann, Y. A. Elnakady, R. M. Wiedmann, *et al.*, *PLoS One*, 2012, **7**, e37416.
- 26 S. Braig, R. M. Wiedmann, J. Liebl, *et al.*, *Cell Death Dis.*, 2014, **5**, e1001.
- 27 R. Bai, G. R. Pettit and E. Hamel, *Biochem. Pharmacol.*, 1990, **39**, 1941–1949.
- 28 H. Benelkebir, S. Marie, A. L. Hayden, *et al.*, *Bioorg. Med. Chem.*, 2011, **19**, 3650–3658.
- 29 B. Long, C. Tao, Y. Li, X. Zeng, M. Cao and Z. Wu, *Org. Biomol. Chem.*, 2020, **18**, 5349–5353.
- 30 H. M. Peltier, J. P. McMahon, A. W. Patterson and J. A. Ellman, *J. Am. Chem. Soc.*, 2006, **128**, 16018–16019.
- 31 J. Lee, S. J. Kim, H. Choi, *et al.*, *J. Med. Chem.*, 2010, **53**, 6337–6354.
- 32 P. H. Nguyen, B. T. B. Hue, M. Q. Pham, *et al.*, *New J. Chem.*, 2023, **47**, 7622–7631.
- 33 H. T. B. Bui, K. M. Do, Q. V. Hong, *et al.*, *Tetrahedron*, 2024, **156**, 133940.
- 34 H. T. Le, K. M. Do, Q. P. Nguyen, *et al.*, *Chem. Pharm. Bull.*, 2024, **72**, 61–67.
- 35 H. T. B. Bui, Z. P. Htoo, Q. V. Hong, *et al.*, *Chem. Pharm. Bull.*, 2024, **72**, 944–949.
- 36 A. L. Pietkiewicz, Y. Zhang, M. N. Rahimi, M. Stramandinoli, M. Teusner and S. R. McAlpine, *ACS Med. Chem. Lett.*, 2017, **8**, 401–406.
- 37 U. Ilyas, S. Naz, S. U. Zaman, *et al.*, *Pak. J. Pharm. Sci.*, 2021, **34**, 1509–1517.
- 38 Z. Abedi-Jazini, J. Safari, Z. Zarnegar and M. Sadeghi, *Polycycl. Aromat. Compd.*, 2018, **38**, 231–235.
- 39 T. M. Dhameliya, R. Tiwari, A. Banerjee, *et al.*, *Eur. J. Med. Chem.*, 2018, **155**, 364–380.
- 40 K. C. Prakasha, G. M. Raghavendra, R. Harisha and D. C. Gowda, *Int. J. Pharm. Pharm. Sci.*, 2011, **3**, 120–125.
- 41 F. Sylvianingsih, U. Supratman and R. Maharani, *Eur. J. Med. Chem.*, 2025, **290**, 117534.
- 42 N. Purushotham, M. Singh, B. Paramesha, *et al.*, *RSC Adv.*, 2022, **12**, 3809–3827.
- 43 S. S. El-Nakkady, M. M. Hanna, H. M. Roaiah and I. A. Y. Ghannam, *Eur. J. Med. Chem.*, 2012, **47**, 387–398.
- 44 P. V. S. Ramya, S. Angapelly, L. Guntuku, *et al.*, *Eur. J. Med. Chem.*, 2017, **127**, 100–114.
- 45 B. Kuhn, P. Mohr and M. Stahl, *J. Med. Chem.*, 2010, **53**, 2601–2611.
- 46 J. T. Coimbra, R. Feghali, R. P. Ribeiro, M. J. Ramos and P. A. Fernandes, *RSC Adv.*, 2021, **11**, 899–908.
- 47 T. Sakamoto, Y. Koga, M. Hikota, *et al.*, *Bioorg. Med. Chem. Lett.*, 2014, **24**, 5175–5180.
- 48 J. de Vicente, R. Lemoine, M. Bartlett, *et al.*, *Bioorg. Med. Chem. Lett.*, 2014, **24**, 4969–4975.
- 49 A. R. Dwivedi, S. Jaiswal, D. Kukkar, *et al.*, *RSC Med. Chem.*, 2025, **16**, 12–36.
- 50 A. Chaudhuri, S. Haldar, H. Sun, R. E. Koeppe II and A. Chattopadhyay, *Biochim. Biophys. Acta*, 2014, **1838**, 419–428.
- 51 A. Dhiman, R. Sharma and R. K. Singh, *Acta Pharm. Sin. B*, 2022, **12**, 3006–3027.
- 52 T. Mosmann and J. Immunol, *Methods*, 1983, **65**, 55–63.

